Applied Radiation and Isotopes 134 (2018) 79–84

Contents lists available at ScienceDirect

Applied Radiation and Isotopes

journal homepage: www.elsevier.com/locate/apradiso

Development of the Australian Standard for Germanium-68 by two Liquid Scintillation Counting methods

W.M. van Wyngaardt*, M.L. Smith, T.W. Jackson, B. Howe, S.M. Tobin, M.I. Reinhard

Australian Nuclear Science and Technology Organisation, New Illawarra Rd, Lucas Heights 2234, NSW, Australia

HIGHLIGHTS

- ANSTO participated in CCRI(II)-K2. Ge68 comparison.
- Standardised ^{68}Ge/^{68}Ga solution by 4πβ^{+}-γ coincidence extrapolation method.
- Standardised ^{68}Ge/^{68}Ga solution by TDCR method.
- ACRMs being developed for ^{68}Ge and ^{68}Ga in geometries used in nuclear medicine.

ARTICLE INFO

Keywords:
Germanium-68
Gallium-68
Liquid scintillation counting
4πβ^{+}-γ coincidence
TDCR
Traceability
Nuclear medicine

ABSTRACT

In response to the increasing application of ^{68}Ge/^{68}Ga and ^{68}Ga in nuclear medicine, an international comparison of activity measurement of ^{68}Ge in equilibrium with ^{68}Ga was organised. ANSTO standardised the comparison solution by the 4π(LS)β^{+}-γ coincidence extrapolation and TDCR efficiency calculation methods, with excellent agreement between the two results. The primary standard was transferred to the ANSTO Secondary Standard Ionisation Chamber. Internationally traceable Australian Certified Reference Materials (ACRMs) of ^{68}Ge/^{68}Ga can now be prepared in various measurement geometries applied in nuclear medicine.

1. Introduction

^{68}Ge is a pure electron-capture radionuclide, decaying with a half-life of $t_{½}$ = 270.95 (26) days to the ground state of ^{68}Ga ($t_{½}$ = 67.83 (20) min) (Fig. 1, Bé et al., 2013). ^{68}Ga disintegrates by a combination of positron emission (88.88 (41) %) and electron capture (11.11 (41) %), predominantly to the ground state of ^{68}Zn. Five excited levels of ^{68}Zn are also populated, which de-excite primarily by the 1077.35 (5) keV γ (1,0) transition (probability = 3.236 (30) %). Thirteen weak gamma transitions with a combined probability of less than 0.4% are also observed.

The relatively long half-life of ^{68}Ge, combined with the relatively short half-life and high positron emission intensity of its daughter radionuclide, ^{68}Ga, makes ^{68}Ge an ideal candidate for the manufacture of generators that can provide a steady supply of radiopharmaceuticals for Positron Emission Tomography/X-ray Computed Tomography (PET/CT) without the need for an on-site cyclotron. The pioneering work of Razbash et al. (2005) resulted in a new type of ^{68}Ge/^{68}Ga generator becoming available, which provides cationic ^{68}Ga eluates instead of inert ^{68}Ga complexes (Rösch, 2013). This availability of trivalent ^{68}Ga eluates paved the way for the present renaissance of ^{68}Ga, with radiopharmaceuticals being applied in imaging for diagnosis and also in treatment planning through theranostics. In Australia, ARTnet, the clinical imaging trials group of the Australian and New Zealand Society of Nuclear Medicine (ANZSNM) and Australasian Association of Nuclear Medicine Specialists (AANMS) is currently undertaking a prostate cancer imaging study, known as ProPSMA, which involves ^{68}Ga-PSMA PET scanning (ANZCTR, 2017).

^{68}Ge/^{68}Ga also provides a convenient long-lived surrogate for the calibration of instrumentation used in nuclear medicine to measure short-lived PET radionuclides. It is essential to take into account differences between the radionuclide of interest (e.g., ^{18}F) and the surrogate, including the half-life, positron branching ratio and additional photon emissions. Low energy emissions (energy E < 11 keV) related to electron capture decay are generally not detected, but differences between positron endpoint energies need to be considered. For example, the production of annihilation photons in locations away from the position of disintegration, as well as Bremsstrahlung radiation being produced through interaction of positrons with matter could result in variation in instrument response (Woods et al., 2002). Differences in

* Corresponding author.
E-mail address: freda.vanwyngaardt@ansto.gov.au (W.M. van Wyngaardt).

http://dx.doi.org/10.1016/j.apradiso.2017.10.005
Received 6 April 2017; Received in revised form 4 September 2017; Accepted 2 October 2017
Available online 04 October 2017

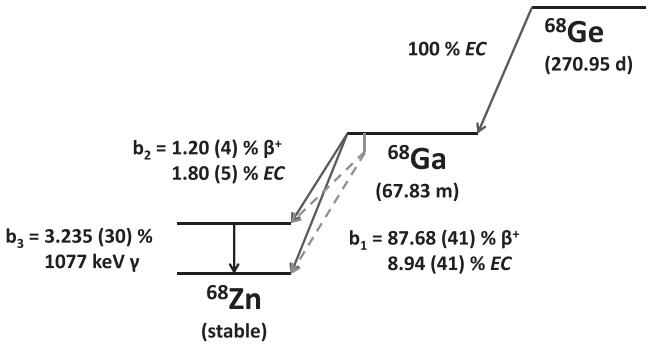

Fig. 1. Simplified decay scheme for ^{68}Ge/^{68}Ga (Bé et al., 2013). The branching probabilities b_1, b_2 and b_3 refer to the two positron emission and gamma emission probabilities respectively.

instrument response can be quantified through direct comparison of activity standards of the radionuclide of interest and the surrogate in the specific measurement geometry or by Monte Carlo simulation.

Quantitative imaging has developed into a powerful tool in Nuclear Medicine that can provide data for oncological staging, treatment planning, monitoring of disease progression and assessment of the efficacy of a new radiopharmaceutical during clinical trials. Often there is the requirement to directly compare PET/CT images that were acquired over time, on different scanner models using different image reconstruction and analysis methods, across different locations, etc. The only way to generate coherent data is to ensure that all radioactivity measurements related to the imaging procedure are directly traceable to national or international activity standards (Zimmerman, 2013). This includes activity measurements on dose calibrators as well as on PET scanners.

In response to the growing need for internationally traceable ^{68}Ge and ^{68}Ga standards, an international comparison of activity measurement of a ^{68}Ge/^{68}Ga solution was organised under the auspices of the Consultative Committee for Ionizing Radiation, Section II (CCRI(II)). As the Designated Institute responsible for maintaining Australia's national standard for radioactivity, ANSTO is a member of CCRI(II) and had the opportunity to participate in the comparison together with sixteen other national radionuclide metrology laboratories. The results are reported by Cessna et al. (in this issue).

This paper describes ANSTO's measurements of the inter-comparison solution by two liquid scintillation counting methods and calibration of Australia's Secondary Standard Ionisation Chamber for ^{68}Ge.

2. Experimental

2.1. Solution used

Special care is required when preparing and handling solutions of ^{68}Ge to prevent activity losses due to volatilisation, precipitation or adsorption (Mirzadeh and Lambrecht, 1996). The pilot laboratory prepared the ^{68}Ge/^{68}Ga inter-comparison solution to also contain approximately 65 μg each of nonactive Ge^{4+} and Ga^{3+} per gram of 0.5 mol/L HCl. They had previously demonstrated that a similar carrier composition provided a ^{68}Ge/^{68}Ga solution that maintained a stable activity concentration for up to 7 years (Zimmerman et al., 2016).

2.2. $4\pi\beta^+$-γ coincidence extrapolation method

The $4\pi\beta^+$-γ coincidence extrapolation method (Bobin, 2007) has been applied to the standardisation of ^{68}Ge by measuring positron emission of the daughter radionuclide ^{68}Ga in coincidence with the associated annihilation photons. Schönfeld et al. (1994), Grigorescu et al. (2004) and Sahagia et al. (2017) each used a proportional counter filled with methane gas at atmospheric pressure to detect positron emissions. They applied a high counting threshold and sources covered with aluminium absorbers to minimize detection of electron capture emissions from ^{68}Ge and ^{68}Ga. The dry sources required for these measurements were prepared by precipitating Germanium as GeS_2. Grigorescu et al. (2004) reported losses of ^{68}Ge of up to 26% when carrier free ^{68}Ge solution was precipitated with H_2S and dried before being sandwiched between plastic foils. In a modified procedure, Sahagia et al. (2017) reported losses of less than 2% when adding $CuSO_4$ to the nonactive carrier solution (containing Ge^{4+} and Ga^{3+} in 0.5 M HCl) and depositing a drop of H_2O saturated with H_2S on top of the ^{68}Ge solution before drying.

Zimmerman et al. (2008), Kulkarni et al. (2017), da Silva et al. (in this issue) and Bobin et al. (2017) used liquid scintillation counting for the beta channel to prevent complications related to the manufacture of dry sources. The detection of electron capture emissions was excluded by threshold discrimination and some of the authors applied different gamma gates to assess the accuracy of a correction for Compton scattering of the 1077 keV γ-ray detected in the NaI(Tl) γ-channel. In a novel application of the $4\pi\beta^+$-γ coincidence method, Bobin et al. (2017) and Marganiec-Gałązka et al. (this issue) prepared counting sources using aqueous carrier solution rather than liquid scintillation cocktail, thereby applying the Cherenkov threshold (~ 260 keV in aqueous solutions) to avoid counting due to electron-capture emissions.

Yamada et al. (2016) standardized ^{68}Ge using the associated $4\pi(\beta^+ + \gamma)$ integral counting method. Here, plastic scintillator sources and a NaI(Tl) well detector were used for measurements. Dry sources were prepared by precipitating Germanium as GeS_2 or $Ge(OH)_2$ and activity losses of 5–8% were reported. The detection inefficiency was evaluated by Monte Carlo simulation using EGS5.

2.2.1. Measurement system

The ANSTO 3-phototube liquid scintillation (LS) counting system described by Qin et al. (2008), with the addition of a 76 mm × 76 mm NaI(Tl) detector, was used for ANSTO's $4\pi\beta^+$-γ coincidence measurements. Data acquisition was performed using the FPGA Acquisition and Software Event Analysis (FASEA) system developed by Steele et al. (2009) (Fig. 2). This system accepts fast NIM logic pulses from a

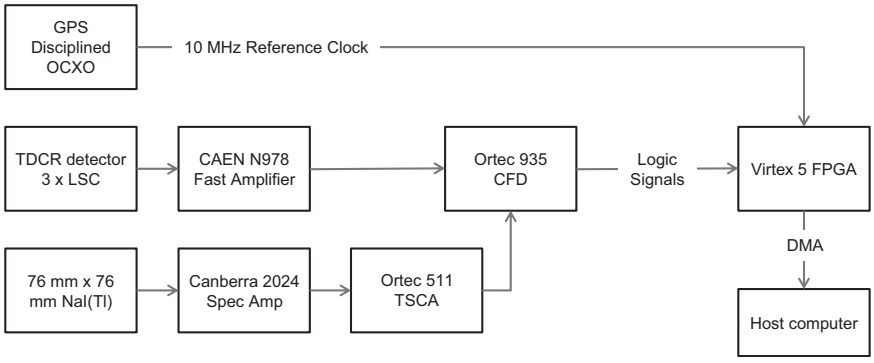

Fig. 2. Schematic diagram of the detection system used for data acquisition (Steele, 2009).

Constant Fraction Discriminator (CFD). Each time a pulse is detected on an input channel the time that this event occurred is transferred via high speed Direct Memory Access (DMA) communication link to the host computer, along with a tag identifying which channel(s) was responsible for triggering the event. Time stamps are provided by an internal 64 bit counter operated at 200 MHz, with time and frequency references supplied by a 10 MHz reference signal coupled to a GPS disciplined oven controlled crystal oscillator (OCXO).

Software developed in Microsoft Visual Basic by Steele et al. (2009) was used to extract single and coincidence count rates from the recorded data. The software shifted the γ-channel time stamps by −17.77 μs to synchronise the LS and γ-channels, while ensuring that all coincidences started with the detection of an event in the LS channel. A resolving time of τ_R = 300 ns was optimal for the detection of LS-γ coincidences, while the LS count rate was insensitive to variation in τ_R between 40 and 400 ns. An extending deadtime of τ_D = 50 μs was applied and the live time used to calculate count rates.

2.2.2. Sources prepared

Counting sources were prepared by dispensing accurately weighed aliquots of radionuclide solution into 10 ml liquid scintillation cocktail contained in 20 ml low-K Wheaton glass vials. The scintillation cocktail used was Ultima Gold from PerkinElmer to which 3 ml of nonactive carrier (96 μg/g Ge^{4+} + 86 μg/g Ga^{3+} in 0.5 mol/L HCl) had been added per litre of Ultima Gold to aid with source stability. Four sources of 12–15 mg each were prepared directly from the inter-comparison master solution. 10 ml of liquid scintillation cocktail was used to prepare a blank for background measurements. Variation in volume and chemical composition between the counting sources and the blank were considered negligible and no additional carrier was added to the blank to match the chemistry.

2.2.3. Measurements and results

The LS channel was set up with the lowest detection threshold at about 20 keV to allow the detection of positron decay of ^{68}Ga but exclude emissions related to electron capture decay from both ^{68}Ge and ^{68}Ga. The LS count rate N_β for a source of activity N_0 can therefore be expressed by

$$\frac{N_\beta}{N_0} = (b_1 + b_2)\varepsilon_\beta, \tag{1}$$

where b_1 and b_2 are the positron branching ratios given in Fig. 1 and ε_β is the positron detection efficiency. Four sources and a blank were counted for five repeats of 400 s real time at each of nine LS efficiency points. The LS detection efficiency was varied between 0.97 − 0.70 by threshold discrimination.

For the NaI(Tl) γ-channel a window was set over the 511 keV full energy peak. The γ-count rate N_γ is predominantly made up of contributions from annihilation photons detected with an efficiency ε_{ann}, and a small contribution from Compton-scattered 1077 keV photons (emission intensity b_3 given in Fig. 1) detected with an efficiency $\varepsilon_{\gamma 1077}$, so that

$$\frac{N_\gamma}{N_0} = (b_1 + b_2)\varepsilon_{ann}\left(1+\frac{b_3}{(b_1 + b_2)}\frac{\varepsilon_{\gamma 1077}}{\varepsilon_{ann}}\right). \tag{2}$$

The coincidence count rate N_C is made up of positrons in coincidence with annihilation photons or Compton-scattered 1077 keV γ-rays. The latter coincidences are only possible for the b_2 branch, so that

$$\frac{N_C}{N_0} = (b_1 + b_2)\varepsilon_\beta \bullet \varepsilon_{ann}\left(1+\frac{b_2}{(b_1 + b_2)}\frac{\varepsilon_{\gamma 1077}}{\varepsilon_{ann}}\right). \tag{3}$$

The measurement data was plotted as $\left(\frac{N_\beta N_\gamma}{N_C}\right)$ vs. $\left(\frac{N_\gamma}{N_C}-1\right)$ and extrapolated to $\left(\frac{N_\gamma}{N_C}-1\right) = 0$ (Fig. 3). It follows from

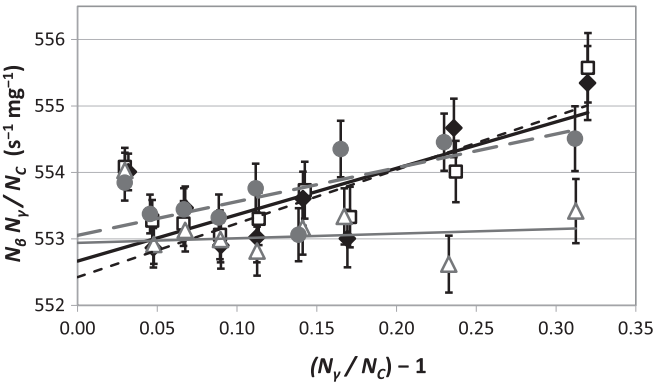

Fig. 3. Plot of weighted linear regression to the eight lowest efficiency points for each of four sources. Error bars indicate statistical uncertainties at k = 1. The highest efficiency points included some electron capture emission and these points were excluded from the regression.

$$\left(\frac{N_\gamma}{N_C}-1\right) = \frac{1}{\varepsilon_\beta}\bullet\frac{\left(1+\frac{b_3}{(b_1+b_2)}\bullet\frac{\varepsilon_{\gamma 1077}}{\varepsilon_{ann}}\right)}{\left(1+\frac{b_2}{(b_1+b_2)}\bullet\frac{\varepsilon_{\gamma 1077}}{\varepsilon_{ann}}\right)}-1, \tag{4}$$

which simplifies to

$$\approx\frac{1}{\varepsilon_\beta}\left(1+\frac{(b_3 - b_2)}{(b_1 + b_2)}\bullet\frac{\varepsilon_{\gamma 1077}}{\varepsilon_{ann}}\right)-1, \tag{5}$$

that

$$\varepsilon_\beta = 1+\frac{(b_3 - b_2)}{(b_1 + b_2)}\bullet\frac{\varepsilon_{\gamma 1077}}{\varepsilon_{ann}} \tag{6}$$

at the Y-intercept. The source activity follows from Eqs. (1) and (6)

$$N_0 = \frac{N_{\beta(intercept)}}{(b_1 + b_2)\bullet\left(1+\frac{(b_3-b_2)}{(b_1+b_2)}\bullet\frac{\varepsilon_{\gamma 1077}}{\varepsilon_{ann}}\right)} = \frac{N_{\beta(intercept)}}{k_1\bullet k_2} \tag{7}$$

The first term (k_1) in the denominator accounts for the positron/electron capture branching ratio, while the second term (k_2) corrects for additional counts in the γ-channel from 1077 keV photons associated with the electron capture branch. A lower limit for the ratio $\left(\frac{\varepsilon_{\gamma 1077}}{\varepsilon_{ann}}\right)$= 0.0589 ± 0.0059 was determined by comparing the NaI(Tl) count rate in the γ-window of a ^{60}Co source of known activity (E_γ= 1173.2 and 1332.5 keV) with the same count rate for a ^{68}Ge source. The uncertainty specified for the ratio was estimated from counting statistics, uncertainty of the source activities and the difference between the photon efficiencies of ^{60}Co and ^{68}Ga due to the different photon energies. Values determined for the correction factors were k_1= 0.8888 ± 0.0042 and k_2= 1.0013 ± 0.0010.

An additional correction factor $k_3 = 1+\frac{(b_3-b_2)}{(b_1+b_2)}\bullet P_{\gamma 1077}$ = 1.0014 ± 0.0020 was determined to account for additional counts in the LS channel due to interaction of the 1077 keV γ-rays associated with the electron capture branch. The interaction probability for a γ-ray of 1077 keV with the LS was calculated using the Monte Carlo program Monty (Simpson, 1994) as $P_{\gamma 1077}$= 0.0614 ± 0.0012. The final source activity was calculated from

$$N_0 = \frac{N_{\beta(intercept)}}{k_1\bullet k_2\bullet k_3} \tag{8}$$

and provided the activity concentration of the inter-comparison solution as C_A= 620.2 (34) kBq/g on the comparison reference date of 14 November 2014. The detailed uncertainty budget is provided in Table 1.

Table 1
Uncertainty budget for $4\pi\beta^{+}$-γ coincidence counting measurements.

Uncertainty component	Relative uncertainty (%)	Comment
Counting statistics	0.03	Statistical analysis of 4 values
Weighing	0.10	Weighing and solution handling
Background	0.05	Statistical variation in background, mostly for the gamma channel
Dead/live time	0.05	Variation of applied dead time and resolving time
Extrapolation of efficiency curve	0.20	Extrapolation to efficiency = 1; variation of points included
Decay correction	0.075	Uncertainty in half-life
Adsorption	0.017	To ampoule
β^{+} / EC branching ratio	0.42	Mostly due to uncertainty in evaluated positron branching ratio
Correction for detection of 1077 keV γ-rays in gamma channel	0.10	Uncertainty in detection efficiency and decay scheme parameters
Correction for detection of 1077 keV γ-rays in LS channel	0.20	Uncertainty in detection efficiency and introduced non-linearity
Combined uncertainty	0.54	$k = 1$

2.3. Triple-to-Double Coincidence Ratio (TDCR) efficiency calculation method

Zimmerman et al. (2008) and Sahagia et al. (2017) have reported applying the TDCR efficiency calculation method (Broda et al., 2007) to the standardisation of ^{68}Ge. Sahagia (2017) applied the same data analysis program *GeGa68* developed by Cassette (2015), which was used in the present work.

2.3.1. TDCR method

With the TDCR method, a source is viewed by a 3-phototube liquid scintillation detection system. The triple coincidence count rate N_t and the logical sum of the double coincidence count rate N_D are recorded simultaneously. If N_0 is the disintegration rate then $N_t = N_0\varepsilon_t$ and $N_D = N_0\varepsilon_D$, where ε_t and ε_D are the triple- and logical sum of the double coincidence detection efficiencies respectively. The efficiencies can be calculated theoretically in terms of a free parameter νA that provides the figure of merit as the number of photons emitted per unit energy deposited in the scintillator. By comparing the ratio of the experimentally measured coincidence count rates with the ratio of the corresponding theoretical efficiencies, νA can be found by solving Eq. (9) iteratively

$$TDCR = \frac{N_t}{N_D} = \frac{\varepsilon_t}{\varepsilon_D}. \tag{9}$$

For a detection system with identical quantum efficiencies for each of the scintillation detectors the theoretical detection efficiencies are given by

$$\varepsilon_t = \int_{spectrum} S(E)(1-e^{-\eta})^3 dE \tag{10}$$

and

$$\varepsilon_D = \int_{spectrum} S(E)(3(1-e^{-\eta})^2 - 2(1-e^{-\eta})^3) dE, \tag{11}$$

where $S(E)$ is the normalized energy spectrum transferred to the scintillator by the radionuclide and

$$\eta = \frac{\nu}{3}\int_0^E \frac{A dE}{1+kB dE/dx} \tag{12}$$

accounts for non-linearity of the light emission process based on the semi-empirical Birks formula (Birks, 1964). A is a free parameter characterising the liquid scintillation cocktail, kB is the semi-empirical Birks parameter and dE/dx describes the linear energy transfer.

The energies transferred to the scintillator were separately calculated by the *GeGa68* program for electron capture decay of ^{68}Ge as well as for decay of ^{68}Ga by electron capture and by two positron emission branches, and the energies summed according to their respective branching ratios (Bé et al., 2013). The calculations were similar to those described in detail by Cassette et al. (2004) for the electron capture radionuclide ^{103}Pd and by Amiot et al. (2012) for ^{64}Cu, which decays by positron and beta minus emission and by electron capture. For electron capture decay a KLM atomic rearrangement model was applied. It was assumed that Auger and conversion electrons, as well as XL emissions, are totally absorbed by the LS cocktail. Cassette (2015) modelled the energy transferred to the LS cocktail by interaction of K_α and K_β X-rays by Monte Carlo simulation using PENELOPE (Savat et al., 2001). Since the ANSTO TDCR detection system was constructed as a replica of the one used by Cassette and the source geometry applied (scintillation cocktail and volume) was the same, Cassette's values for K X-ray energy transfer were applied without modification. Positron spectra were calculated following the Fermi theory using the program SPEBETA (Cassette, 1992). Additional energy deposited in the scintillator by photons related to positron decay was assumed to have a negligible effect on the efficiency calculation for the high positron energies (E_{max} = 1899.1 and 821.7 keV for b_1 and b_2 respectively (Fig. 1)).

2.3.2. Sources prepared

Counting sources were prepared by dispensing accurately weighed aliquots of radionuclide solution into 10 ml liquid scintillation cocktail (Ultima Gold with 3 ml nonactive carrier (96 μg/g Ge^{4+} + 86 μg/g Ga^{3+} in 0.5 mol/L HCl) added per litre of Ultima Gold) contained in 20 ml low-K Wheaton glass vials. For these measurements, the vials had been sand blasted to optimise the detection efficiency of low energy electron capture emissions and reduce effects due to light reflection at the glass-air interface. Two sources of 5–7 mg each were prepared from the master solution and five sources of 50–130 mg each from a 20.07 times dilution. The nonactive carrier was used as the diluent. 10 ml of liquid scintillation cocktail was used to prepare a single blank for background measurements, with no additional carrier added to match the chemistry of the blank with those of the two sets of radionuclide sources.

2.3.3. Measurements and results

TDCR measurements were performed using the same ANSTO 3-phototube LS counting system that was applied for 4πβ-γ coincidence counting. The detection system was set up to measure emissions related to electron capture decay of both ^{68}Ge and ^{68}Ga as well as positron decay of ^{68}Ga. The detection threshold was set just below the single photoelectron peak to ensure applicability of the statistical model applied to calculate the detection efficiency.

The majority of measurements were performed using the FASEA data acquisition system, with confirmatory measurements recorded using the MAC3 unit (Bouchard and Cassette, 2000). During verification of the FASEA system Steele et al. (2009) demonstrated the energy dependence of timing spectra, with widening for low energy emissions such as ^{3}H. Because of the high prevalence of low energy emissions from ^{68}Ge and ^{68}Ga, the capability of the FASEA system to extract coincidence data for various resolving time values was considered particularly valuable.

Five sources prepared from the dilution, together with the blank,

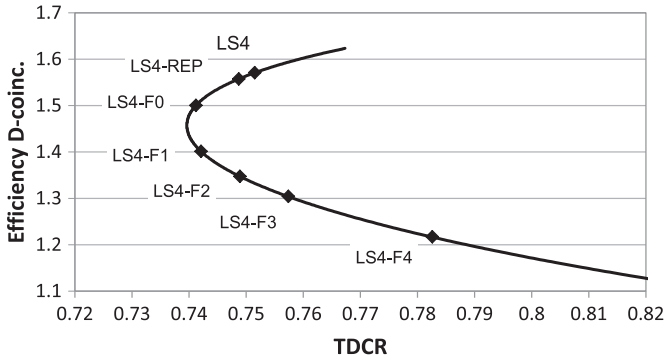

Fig. 4. Plot of the theoretical logical sum of the double coincidence detection efficiency vs TDCR calculated by the *GeGa68* program for $kB = 0.012$ cm/MeV and relative quantum efficiencies for the phototubes of 0.35, 0.30 and 0.35. The markers indicate efficiencies determined from the TDCR values for one source measured without (LS4, LS4-REP) and with five grey filters of increasing light absorption (LS4-F0 to LS4-F4). Measurement by efficiency variation was essential for determination of the efficiency because of the non-monotonic relationship between efficiency and TDCR for electron capture radionuclides.

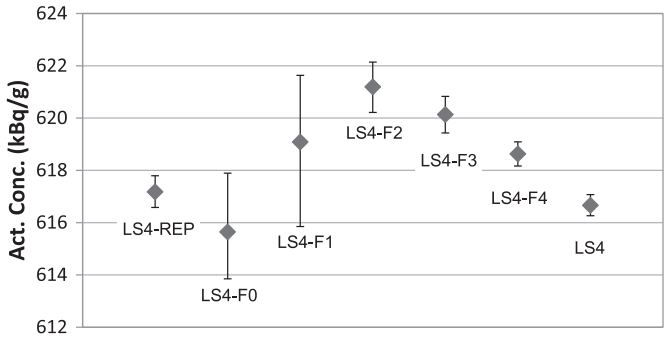

Fig. 5. Results of one source measured without (LS4 and LS4-REP) and with grey filters of increasing light absorption (LS4-F0 to LS4-F4). Variation in the extracted activity concentration indicates some inconsistency in the efficiency calculation model, which was incorporated into the uncertainty budget (Table 2). Only the data from sources counted without grey filters were used to calculate the final activity value. Error bars indicate statistical uncertainties at $k = 1$.

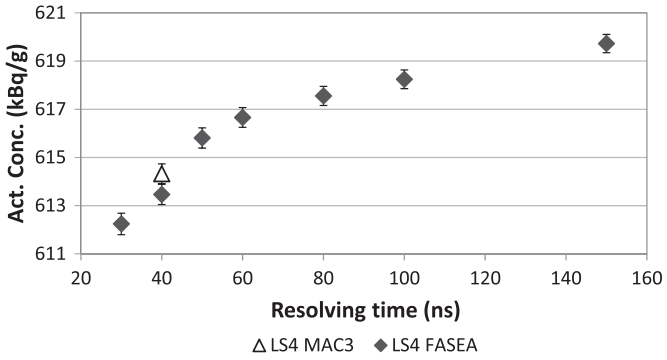

Fig. 6. Effect of variation of resolving time on the result of one source measured with the MAC3 and FASEA data acquisition systems. Data was collected with the MAC3 (unshaded triangle) at a fixed resolving time of 40 ns, while the data collected with the FASEA system (grey diamonds) could be analysed for a range of resolving times. A resolving time of $\tau_R = 60$ ns was applied for the final result. Error bars indicate statistical uncertainties at $k = 1$.

Table 2
Uncertainty budget for TDCR measurements.

Uncertainty component	Relative uncertainty (%)	Comment
Counting statistics	0.15	Statistical analysis of the results from 5 sources
Weighing	0.10	Balance calibration, weighing and preparation of dilution
Background	0.03	Statistical variation of background
Dead/live time	0.10	$\tau_D = 50 \pm 10$ µs
Resolving time	0.30	$\tau_R = 60 \pm 20$ ns
Decay data	0.38	Variation of decay scheme parameters according to evaluated decay data
Decay correction	0.055	Uncertainty in half-life
Adsorption	0.017	To ampoule
Efficiency dependence	0.40	Efficiency dependence on activity concentration
Adsorption	0.12	To scintillation vial
Combined uncertainty	0.68	$k = 1$

were each counted for 5 repeats of 450 s real time using the FASEA data acquisition system. One of the dilution sources and a blank were measured at five additional efficiency points (for 3 repeats of 450 s real time each) to aid with determination of the detection efficiency from the TDCR ratio (Figs. 4 and 5). Efficiency variation was performed by fitting grey filters of different transparencies around the outside of sources. In addition, the two sources prepared from the master solution, one source prepared from the dilution as well as the blank, were each counted for 5 repeats of 300 s live time using the MAC3 data acquisition system. No additional efficiency variation measurements were performed using the MAC3.

All data was initially analysed for an extending deadtime of τ_D= 50 µs and a resolving time of τ_R= 40 ns as these were the settings applied by the MAC3 unit. The activity concentration for the master solution averaged for all measured sources was identical for both systems, with C_A= 615.8 (4) kBq/g, although a 0.13% discrepancy was observed for the one source measured using both acquisition systems (Fig. 6). The uncertainty reported here is from counting statistics only.

The FASEA data were then analysed for the same deadtime τ_D= 50 µs and for resolving times between τ_R= 30 and 150 ns. The data for one of the sources is presented in Fig. 6. The experimental data indicated that a resolving time of τ_R= 60 ns provided an optimal compromise between coincidence losses at short resolving times and inclusion of accidental coincidences at longer resolving times, and this resolving time was applied for the calculation of ANSTO's final TDCR result of C_A= 619.0 (42) kBq/g on the comparison reference date of 14 November 2014. The influence of the resolving time on the activity was taken into account in the uncertainty budget, which is provided in Table 2.

During preparation of this manuscript the uncertainties for counting statistics and the resolving time were reassessed and modified from the values that were reported for the inter-comparison. The uncertainty for counting statistics was increased from 0.05% to 0.15% and the uncertainty due to the resolving time was increased from 0.15% to 0.30%. These adjustments resulted in a slight increase in the combined uncertainty for the TDCR measurements from 0.61% to 0.68%.

2.4. Calibration of the Secondary Standard Ionisation Chamber (SSIC)

An accurately weighed aliquot of approximately 3.6 g of the inter-comparison master solution was transferred to a standard BIPM/NIST type glass ampoule and used to develop a calibration factor for the Australian Secondary Standard Ionisation Chamber (SSIC) (Urquhart, 1986). This is a TPA Mk II ionisation chamber filled with Argon gas at a pressure of approximately ~ 2030 kPa, operated at a bias of 520 V. Current output is measured using a Keithley 6517 A electrometer. The ampoule was measured for 25 sets of 100 measurements each on two separate occasions. Background measurements were recorded as 50 sets of 100 measurements each. Stability measurements (25 sets of 100 measurements) were similarly performed using two sealed ^{226}Ra sources with activities of 821 and 19 100 kBq respectively. The weaker

Table 3
Uncertainty budget for SSIC calibration.

Uncertainty component	Relative uncertainty (%)	Comment
Source activity	0.55	Primary standard by $4\pi\beta^+$-γ coincidence counting and mass of solution
Counting statistics	0.01	Standard deviation of the mean for 25×100 current measurements
Background	0.01	Statistical variation of background
Repeatability	0.10	Standard deviation from two repeat measurements
Stability correction	0.10	Variation between two ^{226}Ra corrections
Non-linearity	0.30	Non-linearity in SSIC response between current range for factor development (33 pA) and standard measurement range (> 700 pA)
Combined uncertainty	0.65	$k = 1$

radium source, which provided a current output similar to that of the ^{68}Ge standard source, was used to determine the radium stability correction applied. The stronger radium source provided a current output in the standard SSIC measurement range, and this variation was taken into account in the uncertainty budget (Table 3). The calibration factor determined was $i_c = 28.96$ (19) pA/MBq. Work is under way to study and improve the SSIC measurement procedures to reduce uncertainties related to non-linearity and stability of the SSIC response.

3. Conclusions

The Australian standard for ^{68}Ge was developed and international measurement equivalence established through ANSTO's participation in the CCRI(II)-K2.Ge-68 key comparison. ANSTO reported results of 620.2 (34) and 619.0 (38) kBq/g for standardisation of the inter-comparison solution by the 4π(LS)β^+-γ and TDCR methods respectively. The results obtained by the two LSC methods agree to within 0.2%, well within the uncertainties specified. ANSTO selected the result of 4π(LS)β^+-γ coincidence counting for equivalence purposes. This value shows excellent agreement with the Comparison Reference Value (CRV) of 621.7 (11) kBq/g (Cessna at al., in this issue).

The standard for ^{68}Ge was transferred to the Australian SSIC through the development of a calibration factor for the geometry of 3.6 ml in a standard ampoule. In addition, Australian Certified Reference Materials (ACRMs) for ^{68}Ge in various measurement geometries applied in nuclear medicine are being developed by ANSTO Radionuclide Metrology. Standards of ^{68}Ge in equilibrium with ^{68}Ga can be used directly to calibrate ionisation chambers and radionuclide dose calibrators for ^{68}Ga as the low energy emissions of ^{68}Ge ($E < 11$ keV) don't provide a measureable response. However, Bremsstrahlung radiation produced through interaction of high energy ^{68}Ga positrons ($E_{max} = 1899$ and 821.7 keV) with source and detector material results in significant geometry dependence when measuring ^{68}Ga in an ionisation chamber. For example, differences in activity concentration of up to 4.8% were observed when using the same calibration setting to measure ^{68}Ga in a glass vial and a plastic syringe (van Wyngaardt, in preparation). It is therefore essential to develop calibration settings for specific measurement geometries applied with direct traceability to national/international standards.

Acknowledgements

The authors wish to thank Philippe Cassette from LNE-LNHB for sharing his *GeGa68* TDCR data analysis program with us, and also Jeff Cessna from NIST for organising the inter-comparison.

References

Amiot, M.N., Bé, M.M., Branger, T., Cassette, P., Lépy, M.C., Ménesguen, Y., Da Silva, I., 2012. Standardisation of ^{64}Cu using an improved decay scheme. Nucl. Instrum. Meth. A 684, 97–104.

ANZCTR, 2017. Australian New Zealand Clinical Trials Registry, Trial ID ACTRN12617000005358 〈https://www.anzctr.org.au/Trial/Registration/TrialReview.aspx?Id=371669&isReview=true〉 (Accessed 23 May 2017).

Bé, M.-M., Chisté, V., Dulieu, C., Mougeot, X., Chechev, V.P., Kondev, F.G., Nichols, A.L., Huang, X., Wang, B., 2013. Table of Radionuclides, vol. 7, Monographie BIPM-5. Bureau International des Poids etMesures, Sèvres. Also 〈http://www.nucleide.org/DDEP_WG/DDEPdata.htm〉 (Accessed March 2016).

Birks, J.B., 1964. The Theory and Practice of Scintillation Counting. Pergamon Press, Oxford, pp. 185–192.

Bobin, C., 2007. Primary standardization of activity using the coincidence method based on analogue instrumentation. Metrologia 44, S27–S31.

Bobin, C., Thiam, C., Bouchard, J., 2017. Standardization of ^{68}Ge/^{68}Ga using the 4πβ-γ coincidence method based on Cherenkov counting. Appl. Radiat. Isot. http://dx.doi.org/10.1016/j.apradiso.2017.06.027. ISSN 0969-8043.

Bouchard, J., Cassette, P., 2000. MAC3: an electronic module for the processing of pulses delivered by a three photomultiplier liquid scintillation counting system. Appl. Radiat. Isot. 52, 669–672.

Broda, R., Cassette, P., Kossert, K., 2007. Radionuclide metrology using liquid scintillation counting. Metrologia 44, S36–S52.

Cassette, P., 1992. SPEBETA Programme de Calcul du Spectre en Energie des Electrons émis par des Radionucléides Emetteurs Beta. CEA Technical Note (Commissariat à l'Énergie Atomique (CEA), Saclay, France.

Cassette, P., 2015. Personal communication.

Cassette, P., Bé, M.M., Jaubert, F., Lépy, M.C., 2004. Measurement of a ^{103}Pd solution using the TDCR method by LSC. Appl. Radiat. Isot. 60, 439–445.

Cessna, J.T., 2017. Results of an international comparison of activity measurements of ^{68}Ge. Appl. Radiat. Isot (In this issue).

Da Silva, C.J., da Cruz, P.A.L., Iwahara, A., Loureiro, J.S., 2017. ^{68}(Ge + Ga) activity standardization by 4πβ(LS)-γ(NaI(Tl)) anticoincidence counting measurements. Appl. Radiat. Isot (In this issue).

Grigorescu, E.L., Negut, C.D., Luca, A., Razdolescu, A.C., Tanase, M., 2004. Standardization of ^{68}(Ge + Ga). Appl. Radiat. Isot. 60, 429–431.

Kulkarni, D.B., Joseph, L., Anuradha, R., Kulkarni, M.S., Tomar, B.S., 2017. Standardization of ^{68}Ge-^{68}Ga using 4πβ(LS)-γ coincidence counting system for activity measurements. Appl. Radiat. Isot. 123, 6–10.

Marganiec-Gałązka, Justyna, Ole J., Nähle, Kossert, Karsten, 2017. Activity determination of 68Ge/68Ga by means of 4πβ(Č)-γ coincidence counting. Appl. Radiat. Isot. http://dx.doi.org/10.1016/j.apradiso.2017.06.027. ISSN 0969-8043.

Mirzadeh, S., Lambrecht, R.M., 1996. Radiochemistry of germanium. J. Radioanal. Nucl. Chem. 202, 7–102.

Qin, M.J., Mo, L., Alexiev, D., Cassette, P., 2008. Construction and implementation of a TDCR system at ANSTO. Appl. Radiat. Isot. 66, 1033–1037.

Razbash, A.A., Sevastianov, Yu.G., Krasnov, N.N., Leonov, A.I., Pavlekin, V.E., 2005. Germanium-68 row of products. In: Proceedings of the 5th International Conference on Isotopes, 5ICI, Brussels, Belgium, Medimond, Bologna, April 25–29, p. 147.

Rösch, F., 2013. Past, present and future of ^{68}Ge/^{68}Ga generators. Appl. Radiat. Isot. 76, 24-30.

Sahagia, M., Luca, A., Antohe, A., Ioan, M.-R., Cîmpeanu, C., Barna, C., Ivan, C., 2017. Standardisation of a ^{68}(Ge + Ga) solution within the CCRI(II)-K2.Ge-68 key comparison. J. Radioanal. Nucl. Chem. 311, 983–990.

Savat, F., Fernandez-Varea, J.M., Acosta, E., Sempau, J., 2001. PENELOPE, a code system for Monte Carlo simulation of electronic and photon transport. Proceedings of a Workshop, OECD/NEA, November 2001, NEA/NSC/DOC19, ISBN: 92-64-18475-9.

Schönfeld, E., Schötzig, U., Günther, E., Schrader, H., 1994. Standardization and decay data of ^{68}Ge/^{68}Ga. Appl. Radiat. Isot. 45, 955–961.

Simpson, B.R.S., 1994. Monte Carlo Calculation of the γ-ray Interaction Probability Pertaining To Liquid Scintillator Samples of Cylindrically-based Shape (NAC Report NAC/94–04). National Accelerator Center, Faure, South Africa.

Steele, T., Mo, L., Bignell, L., Smith, M., Alexiev, D., 2009. FASEA: a FPGA Acquisition System and Software Event Analysis for liquid scintillation counting. Nucl. Instrum. Methods A 609, 217–220.

Urquhart, D.F., 1986. Calibration and operation of the AAEC working standard of measurement for the activity of radionuclides Part I: The measurement system. AAEC Report AAEC/E627. Australian Atomic Energy Commission, Lucas Heights, Australia.

Van Wyngaardt et al. Dissemination of ^{68}Ga standards to support Australian Nuclear Medicine 2017. in preparation.

Woods, D.H., Baker, M.I., Keightley, J.D., Makepeace, J.L., Pearce, A.K., Woodman, A.P., Woods, M.J., Woods, S.A., Waters, S., 2002. Standardisation of ^{11}C. Appl. Radiat. Isot. 56, 327–330.

Yamada, T., Ishizu, H., Kawada, Y., Yunoki, A., Yano, S., 2016. Activity measurement of ^{68}Ge-^{68}Ga by use of $4\pi(\beta^+ + \gamma)$ integral counting method. Appl. Radiat. Isot. 109, 325–329.

Zimmerman, B.E., 2013. Current status and future needs for standards of radionuclides used in positron emission tomography. Appl. Radiat. Isot. 76, 31–37.

Zimmerman, B.E., Cessna, J.T., Fitzgerald, R., 2008. Standardization of ^{68}Ge/^{68}Ga using three liquid scintillation counting based methods. J. Res. Natl. Inst. Stand. Technol. 113, 265–280.

Zimmerman, B.E., Bergeron, D.E., Fitzgerald, R., Cessna, J.T., 2016. Long-term stability of carrier-added ^{68}Ge standardized solutions. Appl. Radiat. Isot. 109, 214–216.